Journal of Industrial and Engineering Chemistry xxx (2014) xxx–xxx

Contents lists available at ScienceDirect

Journal of Industrial and Engineering Chemistry

journal homepage: www.elsevier.com/locate/jiec

Novel Ag/YVO_4 nanoparticles prepared by a hydrothermal method for photocatalytic degradation of methylene-blue dye

R.M. Mohamed [a,b,c,*], E.S. Aazam [a]

[a] Chemistry Department, Faculty of Science, King Abdulaziz University, P.O. Box 80203, Jeddah 21589, Saudi Arabia
[b] Nanostructured Material Division Advanced Materials Department, Central Metallurgical R&D Institute, Helwan 11421, Cairo, Egypt
[c] Center of Excellence in Environmental Studies, King Abdulaziz University, P.O. Box 80216, Jeddah 21589, Saudi Arabia

ARTICLE INFO

Article history:
Received 5 January 2014
Accepted 3 February 2014
Available online xxx

Keywords:
YVO_4
Ag doping
Visible photocatalyst
Methylene-blue dye degradation

ABSTRACT

A hydrothermal method was used to prepare YVO_4 nanoparticles, and a photo-assisted deposition method was used to load Ag onto the YVO_4. The photocatalytic performances of the prepared photocatalysts were tested by the degradation of methylene-blue dye using visible-light irradiation. The results indicate that the Ag is well-dispersed within the YVO_4, and the surface area of the Ag/YVO_4 is smaller than that of the YVO_4 samples. The sample with 0.3 wt% Ag/YVO_4 has the highest activity for the removal of methylene-blue dye. The 0.3 wt% Ag/YVO_4 can be used five times without the loss of its photocatalytic activity.

1. Introduction

Water is the most vital natural resource for life on our planet. Water can be contaminated with many materials, such as organic pollutants, that can lead to diseases and serious problems. Dyes have been found in most of the industrial effluents because they are chemically stable against natural degradation [1,2]. Organic dyes are used in different industries, such as cosmetics, textiles, food and chemical processing; therefore, organic dyes are commonly present in industrial water effluents [3]. Azo compounds are the most popular (50–70%) synthetic dyes that are used today. Methylene blue belongs to one of the primary classes of commercial dyes, and it is stable in the visible and near-UV ranges of light [4]. Methylene-blue dye is widely used in the textile and photographic industries and in printing [5]. Many methods, such as reverse osmosis, adsorption on activated carbon and ultrafiltration, have been used to remove dyes from industrial or waste-water effluents. The serious disadvantages of these methods are that they are non-destructive, and they transfer dyes from one phase to another [6]. In certain cases, the rate of dye removal is notably slow, and the methods are ineffective. For example, the removal of orange-7 dye by ozonation or chlorination methods is slow, ineffective and expensive [3]. The low activity of these methods may be due to the difficulty of degradation of many dyes due to the presence of complex aromatic structures and their synthetic origin [7,8]. Therefore, we must develop new water-treatment methods to protect our environment. The most effective method for removing phenolics and dyes from industrial waste-water is photocatalysis [9–18]. Titania is the best-known photocatalyst, due to its good photostability, high photoactivity, low price and non-toxicity. TiO_2 has two disadvantages for use as a commercial photocatalyst. The first disadvantage is its wide band-gap, which limits its photocatalytic application to the UV range. The second disadvantage is the agglomeration of ultrafine powders, which decreases the photocatalytic activity. Therefore, many researchers have tried to decrease the band gap by different methods, such as by using mordenite [19], graphene [20,21] and metal doping, for example: Sm [22], F [23], Pt [24,25], Ni [26], rare-earth dopants [27], Ag [28,29], Pd [30,31], Co, Cr, and Ag [32]. Yttrium orthovanadate has a band gap 3.5 eV; therefore, it can be excited by UV light [33,34]. The band gap of $InVO_4$ is smaller than that of YVO_4, and their electronic structures are different [35]. Researchers have tried to prepare yttrium orthovanadate by different methods, such as hydrolyzed-colloid reactions [36], a solution-combustion process [37], hydrothermal processing [38], a microemulsion-mediated method [39], wet chemical methods and solid-state reactions [40–43]. As mentioned above, yttrium orthovanadate absorbs in the UV region. The solar spectrum has 4% UV light and the UV can be absorbed by pure water or clear glass. Therefore, we must modify the band gap of yttrium orthovanadate to convert

* Corresponding author at: Chemistry Department, Faculty of Science, King Abdulaziz University, P.O. Box 80203, Jeddah 21589, Saudi Arabia.
Tel.: +966 540715648; fax: +966 2 6952292.
E-mail address: mhmdouf@gmail.com (R.M. Mohamed).

http://dx.doi.org/10.1016/j.jiec.2014.02.004
1226-086X/

it to the visible region. To the best of my knowledge, there are no published papers that discuss the photocatalytic removal of methylene-blue dye under visible light using Ag/YVO_4. The current paper discusses the preparation of Ag/YVO_4 and the estimation of its catalytic performance for degradation of methylene blue dye.

2. Experimental

2.1. Preparation of composite catalyst

A hydrothermal method was used to prepare Yttrium orthovanadate. We prepared a mixture of $Y(NO_3)_3$ and NH_4VO_4 in which the molar ratio of $Y(NO_3)_3$:NH_4VO_4 was 0.1:1. We dissolved the mixture in propanol and adjusted the pH to a value of 10 by adding NaOH solution (1 M) and subsequently stirring the resulting solution with a magnetic stirrer for 1 h. The resulting solution was placed in a Teflon lined autoclave at 150 °C for 8 h. Next, the autoclave was removed from the oven and left to cool naturally to room temperature. The resulting materials were washed several times with bidistilled water, and then dried at 60 °C for 24 h. PAD-Ag/YVO_4 with different wt% of Ag were prepared by PAD (photo-assisted deposition). Ag metal was doped onto the YVO_4 with an aqueous solution of $AgNO_3$ and a strong UV lamp. The Ag/YVO_4 samples (0.1, 0.2, 0.3, and 0.4 wt% of Ag metal) were dried at 60 °C and were then exposed to H_2-reduction (20 ml min^{-1}) at 50 °C for 2 h.

2.2. Characterization techniques

X-ray diffraction (XRD) analysis was carried out at room temperature with a Bruker axis D8 using Cu Kα radiation (λ = 1.540 Å). The specific surface area was calculated from N_2-adsorption measurements, which were obtained using a Nova 2000 series Chromatech apparatus at 77 K. Prior to the measurements, the samples were treated under vacuum at 100 °C for 2 h. The band gap of the samples was identified by UV–vis diffuse reflectance spectroscopy (UV–vis–DRS), which was performed in air at room temperature in the wavelength range of 200–800 nm using a UV/Vis/NIR spectrophotometer (V-570, JASCO, Japan). Transmission electron microscopy (TEM) was conducted with a JEOL-JEM-1230 microscope, and the samples were prepared by suspension in ethanol followed by ultrasonication for 30 min. Subsequently, a small amount of this solution was placed onto a carbon-coated copper grid and dried before loading the sample into the TEM. X-ray photoelectron spectroscopy (XPS) studies were performed using a Thermo Scientific K-ALPHA, XPS, England. Photoluminescence (PL) emission spectra were recorded with a Shimadzu RF-5301 fluorescence spectrophotometer.

2.3. Photocatalysis experiment

The photocatalytic performance of YVO_4 and PAD-Ag/YVO_4 samples was tested for photocatalytic degradation of methylene-blue dye. A horizontal cylinder annular batch reactor was used for the experiments. A xenon lamp (300 W), covered by a UV filter, was used for irradiation of the photocatalyst. The photocatalytic reaction was carried out at room temperature. The required weights of YVO_4 and PAD-Ag/YVO_4 were suspended in a MB solution (500 ml volume and 100 mg/L concentration). Samples were extracted from the mixture at specific times and analyzed by a UV–vis spectrophotometer (V-570, JASCO, Japan).

The photocatalytic removal efficiency of methylene-blue dye was calculated using the following equation:

$$\text{Photocatalytic removal efficiency}\ (\%) = \frac{C_o - C_t}{C_o} \times 100$$

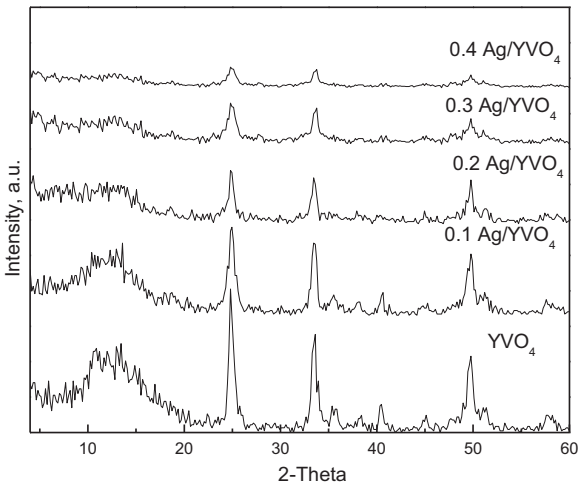

Fig. 1. XRD spectra obtained from YVO_4 and Ag/YVO_4 nanocomposites.

where C_o is the original concentration of methylene-blue dye at time zero and C_t is the concentration of methylene-blue dye at time t.

3. Results and discussion

3.1. Structural, morphological and compositional characterizations

XRD spectra were obtained from YVO_4 and Ag/YVO_4 nanoparticles and are displayed in Fig. 1. The results showed that the YVO_4 and Ag/YVO_4 samples are composed mainly of the YVO_4 structure (JCPDS card no. 17-0341), which indicated that the structure of YVO_4 was retained even after the loading of the Ag by the PAD method. In addition, no peaks were observed for Ag or Ag_2O in the XRD spectra from Ag/YVO_4. This could indicate that the Ag is under the XRD detection limit or that the Ag is dispersed within the YVO_4 phase.

XPS spectra for Ag, from the Ag/YVO_4 nanoparticles, are shown in Fig. 2. The XPS spectra showed that Ag metal was present, with binding energies of 368.1 and 374.2 eV.

TEM images of Ag/YVO_4 nanoparticles are displayed in Fig. 3. The results show that the Ag is well dispersed on the surface of the YVO_4, and the diameters of the Ag nanoparticles increase with increasing wt% of Ag. In addition, the homogeneity of the Ag increases with the increase in wt% of the Ag from 0.1 to 0.3 wt%. At higher wt% of Ag i.e., 0.4 wt%, the homogeneity of the Ag decreased, which indicates that 0.3 wt% is the optimum wt% of Ag.

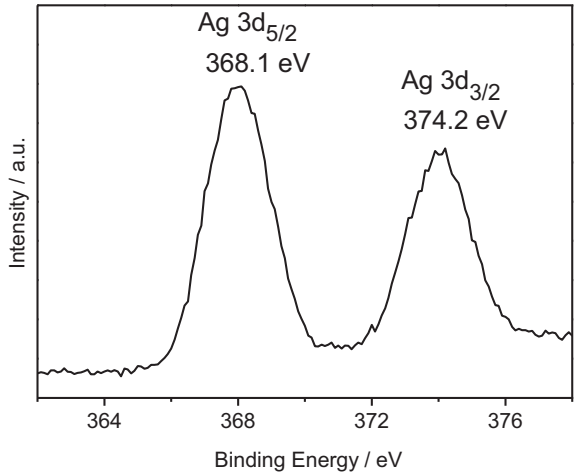

Fig. 2. XPS spectra of Ag in 0.3 wt% Ag/YVO_4.

Please cite this article in press as: R.M. Mohamed, E.S. Aazam, J. Ind. Eng. Chem. (2014), http://dx.doi.org/10.1016/j.jiec.2014.02.004

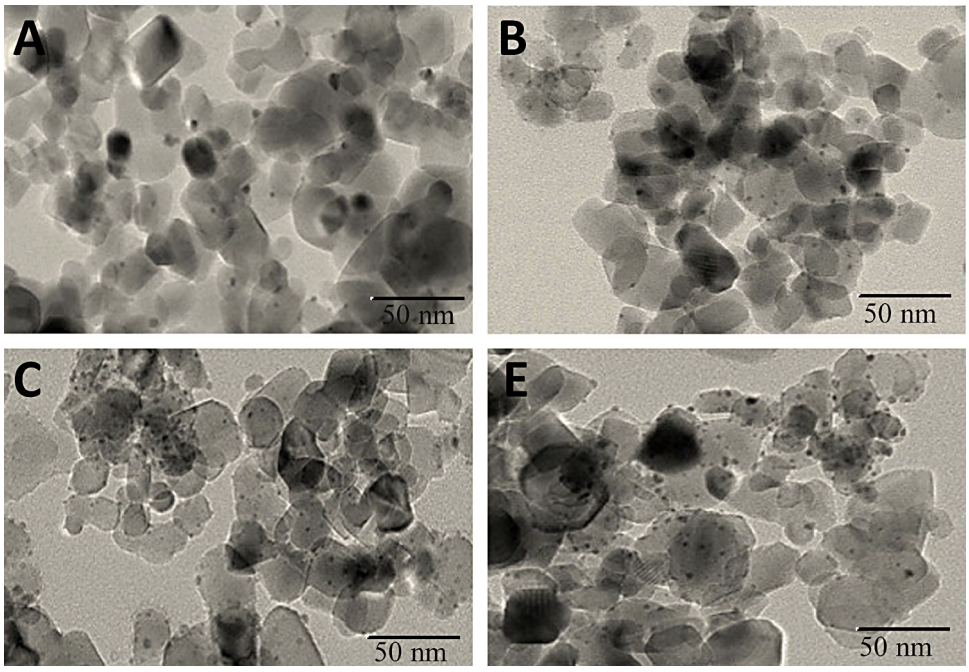

Fig. 3. TEM images of YVO_4 and Ag/YVO_4 nanocomposites, where the wt% of Ag is 0.1 (A); 0.2 (B); 0.3 (C) and 0.4 (D).

Table 1
Texture parameters of YVO_4 and Ag/YVO_4 nanocomposites.

Sample	S_{BET} (m^2/g)	S_t (m^2/g)	S_{micro} (cm^2/g)	S_{ext} (cm^2/g)	V_p (cm^3/g)	V_{micro} (cm^3/g)	V_{meso} (cm^3/g)	r (Å)
YVO_4	113.00	116.00	82.00	31.00	0.310	0.270	0.040	33.00
0.1 wt% Ag/YVO_4	107.00	110.00	80.00	27.00	0.255	0.232	0.023	42.00
0.2 wt% Ag/YVO_4	105.00	108.00	79.00	26.00	0.232	0.210	0.022	52.00
0.3 wt% Ag/YVO_4	103.00	104.00	78.00	26.00	0.225	0.204	0.021	55.00
Ag wt%/YVO_4	98.00	99.00	71.00	24.00	0.208	0.189	0.019	59.00

Note: S_{BET}: BET-surface area; S_t: surface area derived from V_{l-t} plots; S_{mic}: surface area of micropores; S_{ext}: external surface area; V_p: total pore volume; V_{mic}: pore volume of micropores; V_{mes}: pore volume of mesopores; r: mean pore radius.

3.2. Surface area analysis

The S_{BET} of YVO_4 and Ag/YVO_4 nanoparticles were determined. The S_{BET} values were 113, 107, 105, 103 and 98 m^2/g for the YVO_4, 0.1 wt% Ag/YVO_4, 0.2 wt% Ag/YVO_4, 0.3 wt% Ag/YVO_4 and 0.4 wt% Ag/YVO_4, respectively, as shown in Table 1. Furthermore, the total pore volume of the Ag/YVO_4 is smaller than that of the YVO_4 samples. This suggests that some of the pores were blocked by the Ag doping.

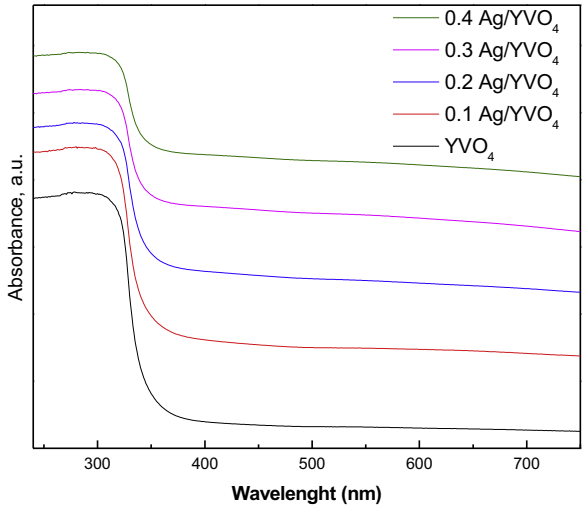

Fig. 4. UV–vis absorption spectra of YVO_4 and Ag/YVO_4 nanocomposites.

3.3. Optical characterization

UV–vis spectra from YVO_4 and the Ag/YVO_4 nanoparticles are displayed in Fig. 4. A red shift toward higher wavelengths, from 418 to 516 nm, was observed as the wt% of Ag was increased. In comparison, YVO_4 absorbs at approximately 383 nm. The following equation was used for calculation of the band gaps of the YVO_4 and the Ag/YVO_4:

$$E_g\,(\mathrm{eV}) = \frac{1239.8}{\lambda}$$

where E_g is the band gap and λ is the wavelength of the absorption edges in the spectrum (nm).

The calculated band-gaps are tabulated in Table 2. The results show that increasing the wt% of Ag up to 0.3 wt% decreases the band gap of the YVO_4. There is no significant effect on the band gap for Ag wt% above 0.3 wt%, i.e., 0.4 wt% as shown in Table 2. This indicates that 0.3 wt% is the optimum wt% of Ag.

Photoluminescence emission-spectra were obtained to study the recombination and separation of photogenerated charge-carriers and the transfer of the photogenerated electrons and holes. Fig. 5 shows the PL spectra from YVO_4 and Ag/YVO_4 nanoparticles. The results indicate that as the Ag wt% is increased up to 0.3 wt% the PL peak intensity decreases. There is no significant effect on PL

Table 2
Band-gap energy of YVO_4 and Ag/YVO_4 nanocomposites.

Sample	Band gap energy, eV
YVO_4	3.3
0.1 wt% Ag/YVO_4	3.0
0.2 wt% Ag/YVO_4	2.8
0.3 wt% Ag/YVO_4	2.5
0.4 wt% Ag/YVO_4	2.4

peak intensity for Ag higher than 0.3 wt%, i.e., 0.4 wt%. The reason of the decrease in PL peak intensity after addition of Ag may be that Ag is acting as a separating agent to separate electrons from holes.

3.4. Photocatalytic performance

The mechanism of photocatalysis starts with the irradiation of semiconductor materials with light to generate electron–hole pairs. The charge carriers are then transferred to the surface of the semiconductor material as in the following equations:

$$YVO_4 + h\upsilon \rightarrow YVO_4(e^-_{CB} + h^+_{VB})$$
$$e^-_{CB}(Ag) \rightarrow e^-_{tr}(Ag)$$
$$e^-_{tr} + O_2(ads) \rightarrow O^-_2$$
$$2e^-_{tr} + 2H^+ + O_2 \rightarrow H_2O_2$$
$$H_2O_2 + e^-_{tr} \rightarrow HO^- + HO^\bullet$$
$$h^+_{VB} + H_2O \rightarrow H^+ + HO^\bullet$$
$$MB + HO^\bullet \rightarrow CO_2 + H_2O$$

Therefore, the photocatalysis produces highly reactive peroxide and hydroxyl radical species. The recombination of electrons and holes is prevented and photocatalytic activity is increased if surface defect states are present. In our Ag/YVO_4 system, Ag prevents electron–hole recombination and increases the photocatalytic activity (Ag acts as a trapping agent).

Fig. 6 shows the photocatalytic activity of YVO_4 and Ag/YVO_4 nanoparticles under visible-light irradiation. The experiment was performed under the following conditions: 0.40 g weight of catalyst, 1000 ml volume of MB dye, 100 ppm MB dye and 7 pH of solution. The results show that the photocatalytic activity of YVO_4 and 0.1 wt% Ag/YVO_4 is notably small due to their broad band-gaps. The photocatalytic activity increased from 67.9 to 100% as the Ag wt% was increased from 0.2 to 0.3, respectively. The photocatalytic activity decreased from 100 to 97% as the Ag wt% was increased from 0.3 to 0.4.

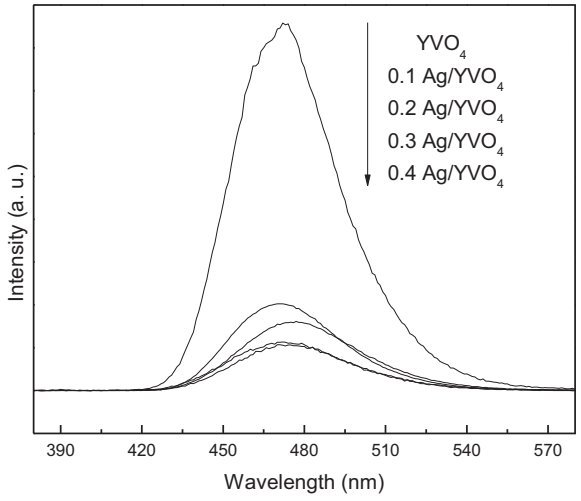

Fig. 5. PL spectra of YVO_4 and Ag/YVO_4 nanocomposites.

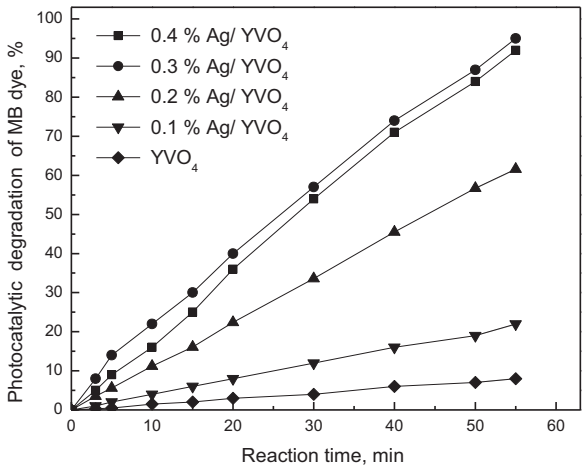

Fig. 6. Effect of wt% of Ag on photocatalytic activity of YVO_4 and Ag/YVO_4 nanocomposites for methylene-blue dye removal.

Fig. 7 shows the effect of catalyst loading on photocatalytic activity. The experiment was performed under the following conditions: 0.40 g of 0.3 wt% Ag/YVO photocatalyst, 1000 ml volume of MB dye, 100 ppm MB dye and 7 pH of solution. The results show that the photocatalytic activity increased from 90 to 100% as the mass of 0.3 wt% Ag/YVO_4 photocatalyst was increased from 0.2 to 0.4 g, with a 60-min reaction time. The reaction time decreased from 60 to 30 min when the mass (that was used) of the 0.3 wt% Ag/YVO_4 photocatalyst was increased from 0.4 to 0.8 g. The reaction time increased again to 40 min when the mass (that was used) of the 0.3 wt% Ag/YVO_4 photocatalyst was increased above 0.8 g. Therefore, the optimum amount of 0.3 wt% Ag/YVO_4 photocatalyst is 0.8 g/l.

Fig. 8 shows the effect of the initial methylene-blue dye concentration on photocatalytic activity. The results show that photocatalytic activity increased when the initial MB dye concentration was increased from 10 ppm to 100 ppm. The time required to degrade the dye is increased when the initial dye concentration is increased above 100 ppm. The photocatalytic activity depends on the rate of formation of hydroxyl radicals on the surface of the semiconductor materials and their reaction with the dye. So, an increase in the initial dye concentration from 10 to 100 ppm increases the reaction of the dye molecules with the hydroxyl radicals and thereby increases the photocatalytic activity. A further increase in the initial dye concentration lead to a decrease in the photocatalytic activity due to the shielding of light by the dye molecules.

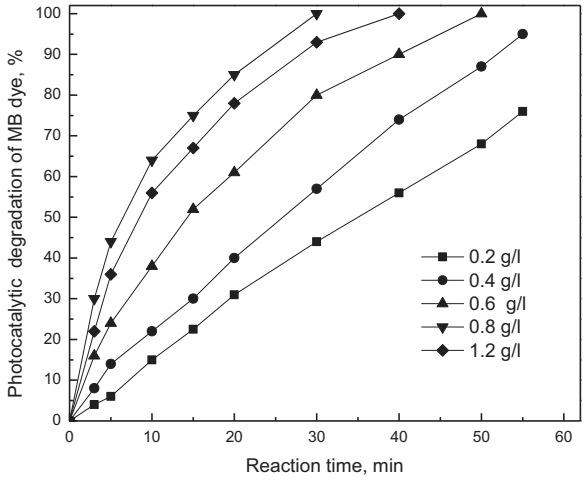

Fig. 7. Effect of loading of 0.3 wt% Ag/YVO_4 on photocatalytic removal of methylene-blue dye.

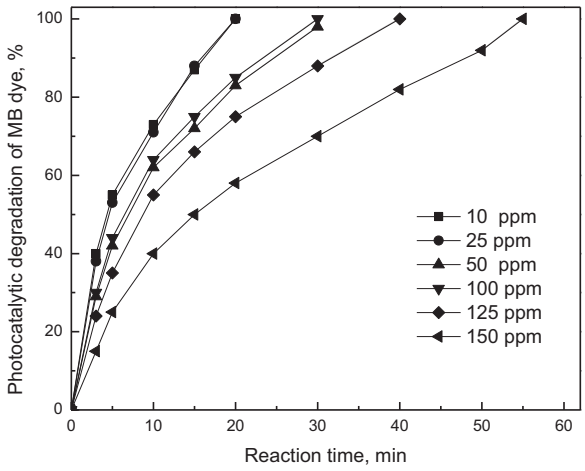

Fig. 8. Effect of initial dye concentration on the photocatalytic degradation of MB dye.

The photocatalytic stability of the Ag/YVO_4 was studied by repeating the photocatalytic experiment five times with a given sample. The photocatalytic performance was found to be 100% during the five cycles, which demonstrated that the photocatalyst was stable for multiple iterations of the photocatalytic process.

4. Conclusions

YVO_4 and Ag/YVO_4 nanoparticles were successfully prepared. Ag/YVO_4 nanoparticles have high photocatalytic activity under visible light. The doping of Ag onto the surface of YVO_4 leads to a shift in the absorption to higher wavelengths, as shown in the UV–vis spectra. The photocatalytic performance of YVO_4 and Ag/YVO_4 nanoparticles for the removal of methylene blue indicate that 0.3 wt% Ag/YVO_4 has the highest photocatalytic activity for water purification. This activity may lead to applications in related fields. The catalyst can be reused with no loss in activity for the first five cycles.

References

[1] C. Fernandez, M.S. Larrechi, M.P. Callao, Trends Anal. Chem. 29 (2010) 1202–1211.
[2] M.A. Ahmed, E.E. El-Katori, Z.H. Gharni, J. Alloys Compd. 553 (2013) 19–29.
[3] K. Rajeshwar, M.E. Osugib, W. Chanmaneec, C.R. Chenthamarakshan, M.V.B. Zanoni, P. Kajitvichyanukul, R. Krishnan-Ayer, J. Photochem. Photobiol. C 9 (2008) 171–192.
[4] W. Nam, J. Kim, G. Han, Chemosphere 47 (2002) 1019–1024.
[5] C. Guo, J. Xu, Y. He, Y. Zhang, Y. Wang, Appl. Surf. Sci. 257 (2011) 3798–3803.
[6] A. Maleki, A.H. Mahvi, M. Alimohamadi, A. Ghasri, Pak. J. Biol. Sci. 9 (2006) 2338–2341.
[7] F. Atmani, A. Bensmaili, N.Y. Mezenner, J. Environ. Sci. Technol. 2 (2009) 153–169.
[8] N. Pasukphun, S. Vinitnantharat, S. Gheewala, Pak. J. Biol. Sci. 13 (2010) 316–324.
[9] F.A. Harraz, O.E. Abdel-Salam, A.A. Mostafa, R.M. Mohamed, M. Hanafy, J. Alloys Compd. 551 (2013) 1–7.
[10] Y. Zhang, J. Wan, Y. Ke, J. Hazard. Mater. 177 (2010) 750–754.
[11] G. Tian, H. Fu, L. Jing, C. Tian, J. Hazard. Mater. 161 (2009) 1122–1130.
[12] S. Sreekantan, L.C. Wei, J. Alloys Compd. 490 (2010) 436–442.
[13] A.M. El-Toni, S. Yin, T. Sato, T. Ghannam, M. Al-Hoshan, M. Al-Salhi, J. Alloys Compd. 508 (2010) L1–L4.
[14] L.F. Velasco, J.B. Parra, C.O. Ania, Appl. Surf. Sci. 256 (2010) 5254–5258.
[15] A.R. Khataee, M. Fathinia, S. Aber, M. Zarei, J. Hazard. Mater. 181 (2010) 886–897.
[16] H.F. Yu, S.T. Yang, J. Alloys Compd. 492 (2010) 695–700.
[17] K. Naeem, F. Ouyang, Physica B 405 (2010) 221–226.
[18] E. Rossetto, D.I. Petkowicz, J.H.Z. dos Santos, S.B.C. Pergher, F.G. Penha, Appl. Clay Sci. 48 (2010) 602–606.
[19] R.M. Mohamed, E.S. Baeissa, J. Alloys Compd. 558 (2013) 68–72.
[20] R.M. Mohamed, Desalin. Water Treat. 50 (2012) 147–156.
[21] W. Shu, Y. Liu, Z. Peng, K. Chen, C. Zhang, W. Chen, J. Alloys Compd. 563 (2013) 229–233.
[22] Y. Cao, Z. Zhao, J. Yi, C. Ma, D. Zhou, R. Wang, C. Li, J. Qiu, J. Alloys Compd. 554 (2013) 12–20.
[23] H. Yan, S.T. Kochuveedu, Li Na Quan, S.S. Lee, D.H. Kim, J. Alloys Compd. 560 (2013) 20–26.
[24] H. Zhang, C. Liang, J. Liu, Z. Tian, G. Wang, W. Cai, Langmuir 28 (2012) 3938–3944.
[25] R. Liu, P. Wang, X. Wang, H. Yu, J. Yu, J. Phys. Chem. C 116 (2012) 17721–17728.
[26] R.M. Mohamed, E.S. Aazam, Chin. J. Catal. 33 (2012) 247–253.
[27] R.M. Mohamed, I.A. Mkhalid, J. Alloys Compd. 501 (2010) 143–147.
[28] R.M. Mohamed, I.A. Mkhalid, J. Alloys Compd. 501 (2010) 301–306.
[29] K. Chen, X. Feng, R. Hu, Y. Li, K. Xie, Y. Li, H. Gu, J. Alloys Compd. 554 (2013) 72–79.
[30] N. Castillo, R. Pérez, M.J. Martínez-Ortiz, L. Díaz-Barriga, L. García, A. Conde-Gallardo, J. Alloys Compd. 495 (2010) 453–457.
[31] M.Y. Abdelaal, R.M. Mohamed, J. Alloys Compd. 576 (2013) 201–207.
[32] R.M. Mohamed, K. Mori, H. Yamashita, Int. J. Nanoparticles 2 (2009) 533–542.
[33] X. Xiao, G. Lu, S. Shen, D. Mao, Y. Guo, Y. Wang, Mater. Sci. Eng. B 176 (2011) 72–78.
[34] A. Huignard, V. Buissette, A.-C. Franville, T. Gacoin, J.-P. Boilot, J. Phys. Chem. B 107 (2003) 6754–6759.
[35] C.-H. Huang, J.-C. Chen, C. Hu, J. Cryst. Growth 211 (2000) 237–241.
[36] S. Choi, Y. Moon, H. Jung, J. Lumin. 130 (2010) 549–553.
[37] S. Ekambaram, K.C. Patil, J. Alloys Compd. 217 (1995) 104–107.
[38] K. Riwotzki, M. Haase, J. Phys. Chem. B 102 (1998) 10129–10135.
[39] L.D. Sun, Y.X. Zhang, J. Zhang, C.H. Yan, C.S. Liao, Y.Q. Lu, Solid State Commun. 124 (2002) 35–39.
[40] A. Huignard, V. Buissette, G. Laurent, T. Gacoin, J.P. Boilot, Chem. Mater. 14 (2002) 2264–2269.
[41] L. Chen, Y. Liu, K. Huang, Mater. Res. Bull. 41 (2006) 158–163.
[42] H. Zhang, X. Fu, S. Niu, G. Sun, Q. Xin, J. Solid State Chem. 177 (2004) 2649–2654.
[43] Y. Li, G. Hong, J. Solid State Chem. 178 (2005) 645–649.